A Topological Glass

Jean-Pierre Eckmann

Département de Physique Théorique et
Section de Mathématiques
Université de Genève
1211 Genève 4, Switzerland

Abstract. We propose and study a model with glassy behavior. The state space of the model is given by all triangulations of a sphere with n nodes, half of which are red and half are blue. Red nodes want to have 5 neighbors while blue ones want 7. Energies of nodes with different numbers of neighbors are supposed to be positive. The dynamics is that of flipping the diagonal of two adjacent triangles, with a temperature dependent probability. We show that this system has an approach to a steady state which is exponentially slow, and show that the stationary state is unordered. We also study the local energy landscape and show that it has the hierarchical structure known from spin glasses. Finally, we show that the evolution can be described as that of a rarefied gas with spontaneous generation of particles and annihilating collisions.

1 Introduction

Our model of a glass can is inspired by an abstraction of a model and its representation found in [1]. Before we introduce our version, and to make contact with that paper, we describe briefly the model of [1]. One starts with a binary mixture of n disks in the plane, with the small disks having radius $\sigma_{\rm s} = 1$ and the large, $\sigma_\ell = 1.4$. The three pairwise additive interactions are given by purely repulsive soft-core potentials of the form

$$\varepsilon \left(\frac{\sigma_a + \sigma_b}{2r} \right)^{12} ,$$

with $a, b \in \{{\rm s}, \ell\}$, $\varepsilon > 0$, and r the distance between the centers of the disks. One assumes the interaction vanishes for $r > 2.25(\sigma_a + \sigma_b)$. Taking periodic boundary conditions, and a relatively tight volume, the authors of [1] found that this system shows the characteristics of a glass when the temperature is sufficiently low.

The part of the analysis which is of interest for the present study has to do with a geometric representation of configurations of this system. One draws in the plane a point for the position of the centers of the disks, and proceeds then to use the Voronoi tessellation. This means that lines are drawn between nearest neighbors in the sample, and their normal bisectors are then used to draw polygons around each particle. These polygons turn out to be mostly pentagons around the small particles and heptagons around the large ones, with a few exceptions as a function of temperature, and by the constraints of Euler's theorem on polygonal domains on surfaces. See Fig. 1.

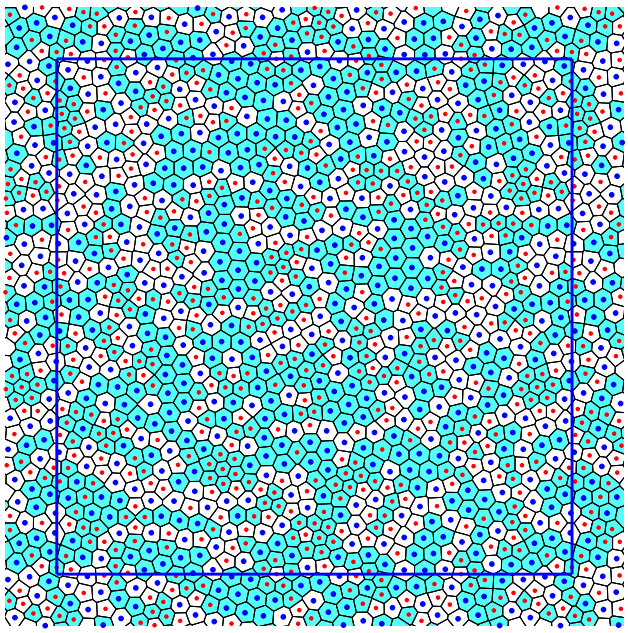

Fig. 1. A Voronoi tessellation (adapted from [1]). The interpretation of the figure is as follows: Blue dots correspond to the positions of the big particles and red dots to the small ones. The polygons are white, for every blue particle in a heptagon and every red particle in a pentagon. All hexagons are in blue-green. There are no other polygons at this temperature ($T = 0.1$, see [1]). The blue line shows the boundary of the domain, which is extended periodically beyond.

In this paper, we consider a purely topological variant of the above model and show it has the properties of a glass. The model is basically obtained by considering instead of the Voronoi tessellation the *dual* graph, which is a triangulation (of the torus). This triangulation is obtained from Fig. 1 by connecting the centers of the particles normally across the edges of the Voronoi tessellation. (The dual graph is a triangulation since each edge of the polygons meets exactly 2 other edges at its end.)

To simplify things further, we consider instead a triangulation $\mathcal{T}$ of the sphere. Given n, the number of "particles," we let $\mathcal{T}$ denote a triangulation of the sphere with n nodes and we let $\mathbb{T}_{n,0}$ denote the set of all such triangulations. By this, one means the set of all combinatorially distinct rooted simplicial 3-polytopes. In particular, a triangulation should not have any "double edges". We further refine the definition, by distinguishing 2 types of nodes in the triangulation: We first number the nodes from 1 to n and then define 2 types of nodes. Those with even index are the "small particles" and those with odd index the "large" ones. This means that the triangulation has the same number of large and small nodes (up to a difference of one). We will also call the two types of nodes two *colors*.

Definition 1.1. *We shall call the odd nodes* blue *and the even ones* red *and will refer to the triangulations as* colored *triangulations.*

Once the colors are assigned, the numbers are again forgotten. The set of all colored triangulations with n nodes will be called $\mathbb{T}_n$. This is our *phase space* and the dynamics is mapping points in this phase space to other points.

As in the original model, we introduce an energy E for each triangulation $\mathcal{T}$:

$$E(\mathcal{T}) = \sum_{i=\text{odd}} (d_i - 7)^2 + \sum_{i=\text{even}} (d_i - 5)^2 \,, \tag{1.1}$$

where d_i is the number of links meeting at node i. Except for the constraint given by Euler, that $\sum_{i=1}^{n} d_i = 6n - 12$, the lower bound of the energy is obviously $E(\mathcal{T}) \geq 0$.

Remark 1.2. The choice of energy is not as "universal" as one could wish. In a way, it would be more adequate to be able to develop a theory which deals with a family of energies, which all have the property that the minima are at again at 5 and 7, but which should somehow be independent of the details of how the errors are weighted. For example, one expects similar results for an energy of the form

$$E(\mathcal{T}) = \sum_{i=\text{odd}} (d_i - 7)^2 + 2 \sum_{i=\text{even}} (d_i - 5)^4 \,.$$

On the positive side, we will see that the hierarchical structure of the energy landscape indeed does not depend on the details of the energies, only one their behavior near the quadratic minima.

We next define a *dynamics* on the set of all triangulations $\mathbb{T}_n$ which is inspired by the motion of the dual to the Voronoi tessellation of the model in [1].

1) Choose a link at random.
2) Consider the two triangles touching that link, say ABC and BCD (having the common link BC). If the link AD exists in the triangulation go back to 1). (This can happen when ABCD form a tetrahedron.)
3) In principle, we want to flip the link BC and replace it by AD, *i.e.*, exchange the triangles ABC and BCD with ACD and ABD. This operation is called a flip [7], or a Gross-Varsted move [5] and it will transform the triangulation $\mathcal{T}$ to a new one $\mathcal{T}'$.
4) If $E(\mathcal{T}') \leq E(\mathcal{T})$ then perform the flip and continue at 1).
5) If $E(\mathcal{T}') > E(\mathcal{T})$ then perform a flip with probability $e^{-\beta(E(\mathcal{T}')-E(\mathcal{T}))}$ and continue at 1). This is of course a typical Monte-Carlo step (at inverse temperature β).
6) Continue at 1).

2 Irreducibility

Having defined precisely the algorithm, we first show that the phase space $\mathbb{T}_n$ is irreducible.

Lemma 2.1. *The action described above defines an irreducible Markov process on $\mathbb{T}_n$ (when $n > 7$). This means that any configuration can be reached from any other configuration.*

Proof. For the case of the uncolored triangulations, $\mathbb{T}_{n,0}$, this is a well-known result [7, 10], see also [3]. In that case, one shows that every triangulation can be transformed by a sequence of flips to the "christmas tree" of Fig. 2. Note that this reduction takes place *without* shifting around the nodes of the outermost triangle. A typical sample move to achieve the reduction of the number of links at the top is shown in Fig. 3.

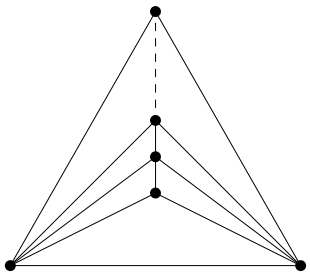

Fig. 2. The Christmas tree. Two nodes are at the bottom, the others (only 4 shown) are in the stem of the tree.

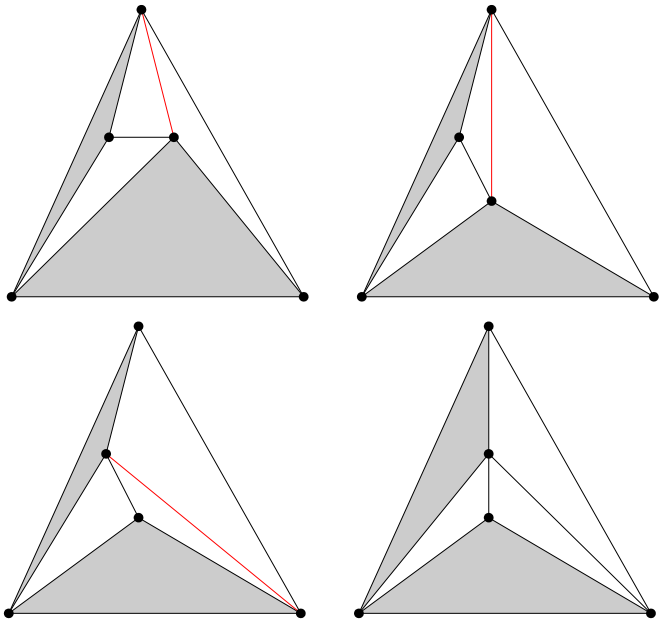

Fig. 3. Reducing the degree at the top of the christmas tree by 1. Note that the gray regions can contain any triangulation. The complete christmas tree is obtained by inductively working "down" from the top to the bottom, once the top node has been reduced to degree 3. The sequence of events is top left, top right, bottom left, and bottom right. The actual flip is done between frame 2 and 3. The other transformations just move the nodes into place for better visibility.

We next show irreducibility in $\mathbb{T}_n$, where the positions of the colors now matter. Since we can move any triangulation to a christmas tree, we therefore only need to show that one can exchange

the places of the colors in the christmas tree. We first show in Fig. 4 how this is done for any two positions on the stem, with the exception of the two bottom ones. Those are handled by the flips shown in Fig. 5. Finally, one can "exchange" colors in the outermost triangle as follows: Observe that the "outermost" triangle is arbitrary since one can declare any triangle of the triangulation of the sphere to be the outermost one. In other words, we can reduce the question to the preceding ones by declaring a new triangle to be the outermost one, bring the triangulation to the christmas tree form and proceeding as before. □

Remark 2.2. One can also show, see [3], that the Markov process defined above is aperiodic, *i.e.*, some power of the transition matrix has only non-zero entries.

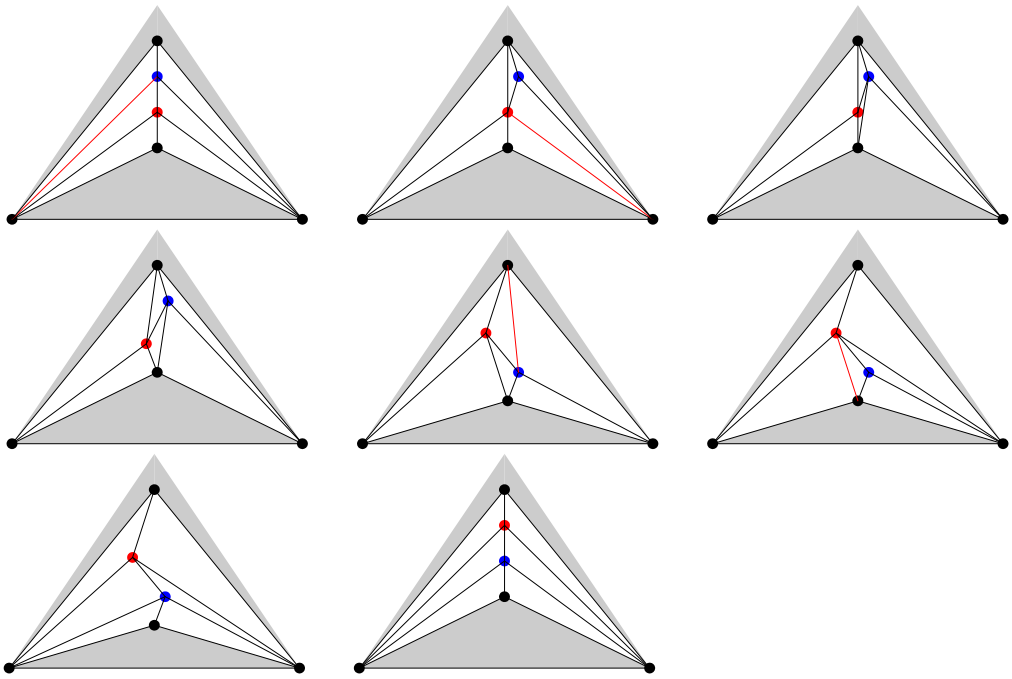

Fig. 4. Exchanging blue and red in the stem of the christmas tree by a sequence of moves. Top to bottom. The actual flips are taking place between frames 1-2, 2-3, 5-6, 6-7. The other transitions are again just moves for better visibility. Note that the shaded regions may contain arbitrary links, in particular, parts of the stem of the tree. Therefore, this sequence shows that any two positions in the vertical stem can be exchanged, except for the bottom 2. Those will be handled in Fig. 5.

Remark 2.3. Note that the energy of the christmas tree (with n nodes) is at least (depending on the distribution of colors)

$$E_{\text{tree}}(n) \geq 2 \cdot (7-(n-1))^2 + (n-3) \cdot (5-4)^2 + 1 \cdot (5-3)^2 = 2n^2 - 31n + 129 \,,$$

when $n \geq 8$. It is important to note that the christmas tree is an "expensive" configuration energy-wise, but very convenient as a topological anchor from which to reach other configurations.

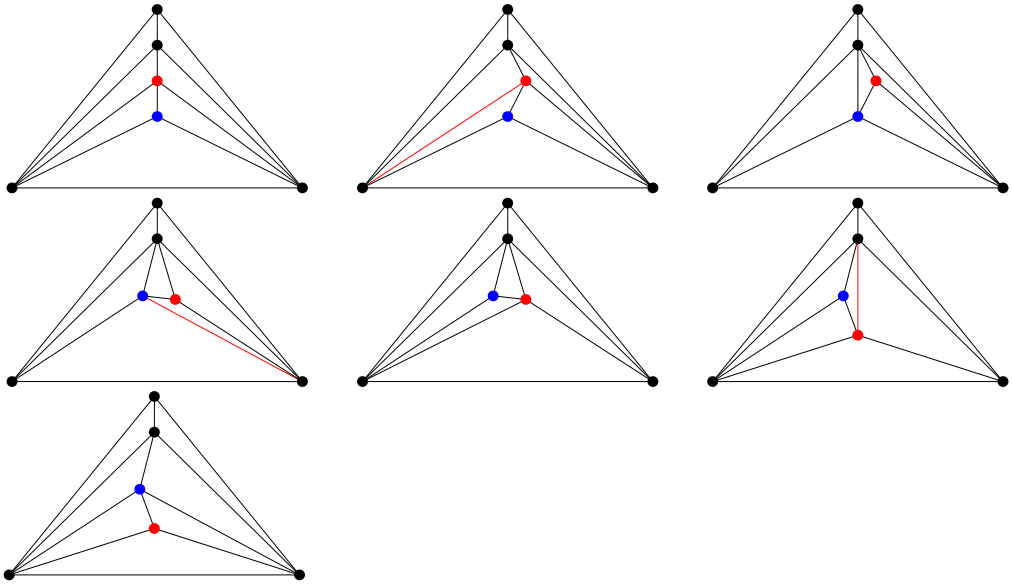

Fig. 5. Exchanging blue and red in the two bottom positions of the christmas stem. Top to bottom. The flips occur between frames 2-3, 4-5, and 6-7.

3 The phase space

In this section, we describe the phase space $\mathbb{T}_n$ of the system. The possible states of our system of triangulations with n nodes is the set $\mathbb{T}_n$ of all possible colored triangulations. The set $\mathbb{T}_n$ has, as we will see, a number of elements which grows like C^n for some constant C. It is thus a discrete space with a finite number of states. To describe the dynamics of flipping in a geometric way, one should view this set as the *dynamical graph* $\mathcal{G}$, in which the nodes are the elements of the set $\mathbb{T}_n$ and two nodes are linked if one can be reached from the other by a flip. (This makes an undirected graph, since one can flip back and forth.) The reader should note that there are two graphs in this discussion: Each triangulation is a graph with n nodes, and $3n-6$ links (by Euler's theorem), while the graph $\mathcal{G}$ has about C^n nodes, and about $3n-6$ links *per node*. This last statement follows because in every state of $\mathbb{T}_n$, one can choose which of the $3n-6$ links of the triangulation $\mathcal{T}$ one wants to flip. However, there will, in general, be somewhat fewer links which are candidates for flipping, because whenever there is a node of degree 3 in the triangulation $\mathcal{T}$ its links can not be flipped (a tetrahedron is unflippable).

In more physical language, comparing with the local degree in $\mathbb{Z}^d$, (which is $2d$), one can say that the "local dimension" of the dynamical graph $\mathcal{G}$ is something like $\mathcal{O}(n)$, while the size of the phase space (the number of nodes in $\mathcal{G}$) is $\mathcal{O}(1)^n$.

Finally, given any two elements in $\mathbb{T}_n$, that is, any two triangulations with n nodes, we will show below that $\mathcal{O}(n^2)$ flips are sufficient to walk on the graph $\mathcal{G}$ from one to the other. Thus, the diameter of the graph $\mathcal{G}$ is at most $\mathcal{O}(n^2)$ while it has $\mathcal{O}(1)^n$ vertices. This means that $\mathcal{G}$ has the "small world" property [11]. It has also small clustering coefficient, since there are very few

triangles in the graph $\mathcal{G}$ (it is difficult to get form a triangulation back to the same triangulation with 3 flips).

In the remainder of this section, we prove these statements. They are well-known for uncolored graphs, so the only task is to prove them for the colored graphs.

We first state two known results for the set $\mathbb{T}_{n,0}$ of uncolored triangulations:

Lemma 3.1. *[8, 7, 6] The number of elements in $\mathbb{T}_{n,0}$ is asymptotically*

$$\left(\frac{256}{27}\right)^{n-3} \frac{3}{16\sqrt{6\pi n^5}} \,. \tag{3.1}$$

The distance between any two uncolored triangulations is at most $6n-30$ flips.

For the case of the colored graphs, with $n_{\rm red} = n_{\rm blue} + c$ and $c \in \{0, 1\}$, that is, about equal number of red and blue nodes, one has

Lemma 3.2. *The number of elements in $\mathbb{T}_n$ is asymptotically bounded above by*

$$2^n \left(\frac{256}{27}\right)^{n-3} \frac{3}{16\sqrt{6\pi n^5}} \,, \tag{3.2}$$

and below by the expression (3.1). The distance between any two colored triangulations in $\mathbb{T}_n$ is bounded by

$$C_1 n^2 + C_2 \tag{3.3}$$

flips with some universal constants C_1, C_2.

Remark 3.3. This result might be compared to glass models on cubes. In that case, one has also the small world property [2]. However, our model is not "trap"-like, since there are no very deep holes but rather very narrow corridors, see also Sect. 7.

Proof. The lower bound in (3.2) is obvious from Lemma 3.1, since there are certainly more triangulations with coloring than without. The upper bound follows by observing that there cannot be more than 2^n different colorings of the nodes of any uncolored triangulation. To estimate the number of steps needed to connect two colored triangulations, we reduce the problem to the uncolored one. Starting from an arbitrary triangulation $\mathcal{T}$ in $\mathbb{T}_n$, we can go to $\mathcal{T}' \in \mathbb{T}_n$ *without respecting the colors*, by "passing through the christmas tree". This needs at most $12n - 60$ flips. However, the colors in the final position might be wrong and they must be reordered. We do this not at the end, but when we are at the christmas tree. Here we use the method described in Fig. 4 and 5. Each permutation of two neighboring colors can be done by at most 4 flips. Since no color has to be moved by more than $n-1$ positions, and there are n nodes we get the bound (3.3) as asserted. □

4 The energies

Up to now, our discussion has been purely topological. But there is also energy. The shortest paths (of length at most $C_1 n^2 + C_2$ as described in Lemma 3.2) to go from $\mathcal{T}$ to $\mathcal{T}'$ are by no means energetically optimal, and optimal paths are difficult to find. We have already seen in Remark 2.3 that the christmas tree has energy $\mathcal{O}(n^2)$. The minimal energy of the model is clearly 0, by (1.1). However, this energy can not be quite reached, because of Euler's theorem. We have the following, probably non-optimal result:

Lemma 4.1. *For every $n = 18 + 12k$ with $k \in \mathbb{N}$, there is a triangulation $\mathcal{T}$ in $\mathbb{T}_n$ (with an equal number of red and blue nodes) whose energy $E(\mathcal{T})$ is between 6 and 54.*

Corollary 4.2. *There is a constant C such that for every n there is a triangulation $\mathcal{T} \in \mathbb{T}_n$ (with the number of red and blue nodes differing by at most 1) such that $E(\mathcal{T}) \le C$.*

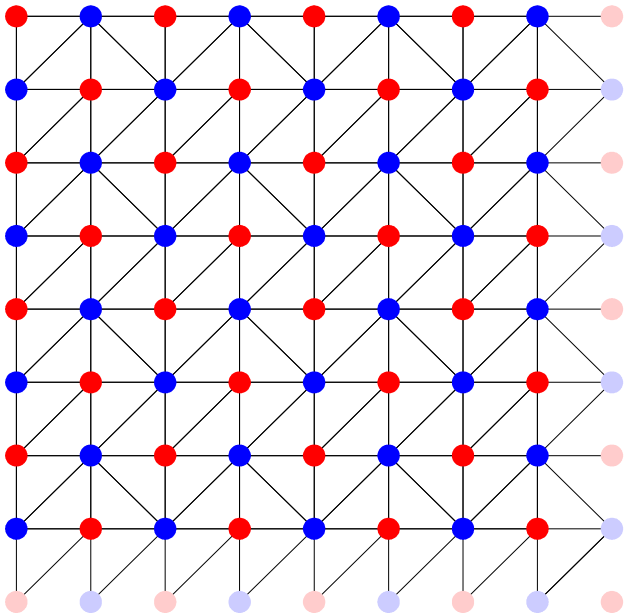

Fig. 6. A triangulation of the torus with 64 nodes and energy 0. We show the 64 nodes and the periodic extension (softer colors).

Remark 4.3. Note that the statements above are by and large independent of the choice of the function E, provided it has its local minima at 5 and 7. Of course, the constants will depend on the details of E but the basic facts will not. What will change, however, is, *e.g.*, the highest possible energy. In our case, it is $\mathcal{O}(n^2)$ but for potentials which grow faster it will be higher.

Remark 4.4. One can also study triangulations of the torus (where the Euler characteristics is 0). In that case, it is easy to see, and in fact shown in Fig. 3 of [1], that there is a state of energy 0 when n is a multiple of 4. This state is a regular arrangement of nodes of degree 5 and 7 (see Fig. 6). Note that flipping all the links connecting blue nodes in the 2nd column will exchange blue and red there and will generate another configuration of energy 0. Since this can be done for all even columns independently, the degeneracy of the ground state of torus triangulations with $n = 4k$ nodes is at least about $2^{\sqrt{k}}$, which makes it quite degenerate. One can play the same game with horizontal rows, but this does not change the square root behavior of the exponent.

Proof (of Lemma 4.1). The proof is by construction. In Fig. 7 we show a triangulation which has 18 nodes, and energy E between 6 (which seems to be the minimal possible energy) and 54. Note that the shaded triangle has the same number of internal links from its corners than the outermost triangle (namely 6). Therefore, we can repeat the construction recursively in the interior triangle by adding another 12 nodes (6 blue and 6 red), *i.e.*, the shaded triangle will look like the original one. Its 3 black nodes will become red. Therefore, the number of black dots will not increase, and we see that for $k \in \mathbb{N}$ there is a triangulation with $18 + 12k$ nodes, with energy between 6 and 54, as asserted. The corollary follows immediately: If $n = 18 + 12k + \ell$ with $0 \leq \ell \leq 11$, we just do the construction for $n' = 18 + 12k$ nodes and add the additional ℓ nodes inside the innermost (black) triangle, and connecting them to make a triangulation. This subgraph and its connections to the black nodes will increase the energy by some finite, k-independent amount. □

Remark 4.5. The bounds of Lemma 4.1 are not optimal. For better values, see also the numerical studies of Sect. 6.

We next give a bound on the degeneracy of the energy levels. Given n, one can ask about the number $N(n, E)$ of triangulations of $\mathbb{T}_n$ of energy $\leq E$, and of course, one can ask about their distribution in the limit $n \to \infty$. Here, we only have a lower bound on N, which is certainly not optimal. But this bound will show that for intermediate energies $N(n, E)$ grows at least like $C(E)^n$ as $n \to \infty$.

Lemma 4.6. *There are constants $C_* > 1$ and $E_* > 0$ such that the following holds. For every sufficiently large n and every $100 < E < E_* n$ one has the lower bound*

$$N(n, E) \geq C_*^E \,. \tag{4.1}$$

Remark 4.7. The inequality (4.1) can also be interpreted by saying that the number of states with energy εn and $\varepsilon < E_*$ is at least

$$N(n, \varepsilon n) \geq C_*^{\varepsilon n} \,.$$

This should be compared to the growth rate of the number of triangulations in $\mathbb{T}_n$ which is also of the form $\mathrm{const.}^n$.

Proof. We give again a constructive proof, with no attempt to optimality. We begin with a graph G_m of the type of Fig. 7 with $m = 18 + 12k$ nodes. In every triangle of G_m we may insert a

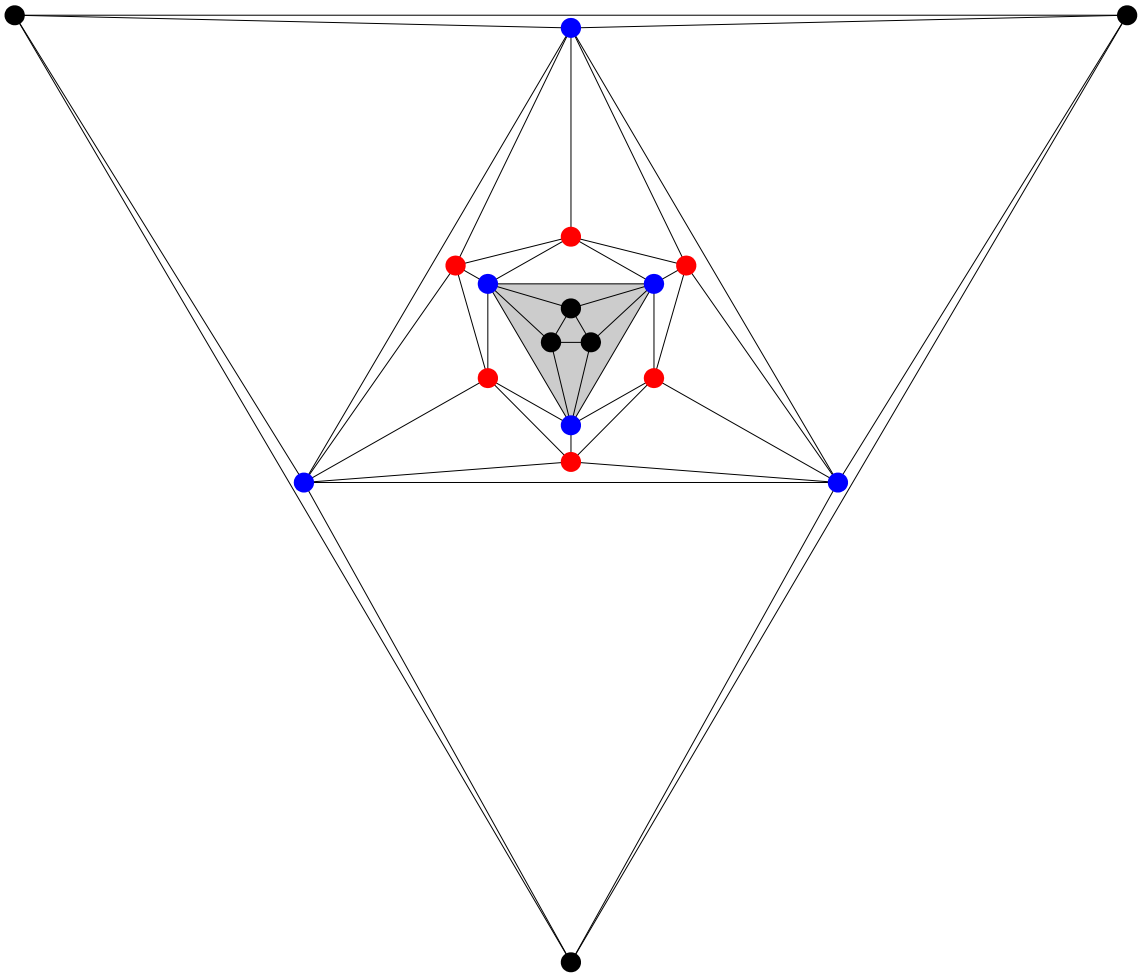

Fig. 7. A triangulation $\mathcal{T}$ with 18 nodes and energy $E(\mathcal{T}) \leq 54$. The blue nodes have degree 7 and the red ones have degree 5. The black ones have degree 4, which means that the energy of the triangulation is at least $6 \cdot (5-4)^2 = 6$ and at most $6 \cdot (7-4)^2 = 54$.

graph H which we now describe. The graph H is of the following form: First extend the triangle "inward" as shown in the leftmost panel of Fig. 8 (the triangle with the red point). Then the inner gray triangle is filled with the triangulation of Fig. 7, *i.e.*, with G_1. Finally in the innermost triangle of Fig. 7 we draw a christmas tree by adding 2 vertices. This tree will break the rotation symmetry of Fig. 7. The whole construction adds 20 nodes to the original graph G_m, for every insertion of H (3 nodes in the first step, another 15 to place Fig. 7 and 2 more for the tree). Since there are $2m-4$ triangles in the original graph there can be at most $2m-5$ insertions of H, namely one per original triangle (we do not insert into the outside of the basic triangle).

Note now that rotating the interior graphs in H as shown in the 3 panels of Fig. 8 will create a different graph for each rotation of each of the inserted H, except perhaps for one overall rotation.

All these graphs have the same energy. Thus, if there are p insertions of H there will be 3^p graphs with the same energy and the same n.

We next give an upper bound on the change of energy when inserting p of these graphs H. Inserting a triangle as in the left panel of Fig. 8 will increase the degree at each of the three nodes by 1. Since the original degree was at most 7, the new degree is at most 14 and hence, for every inserted H this contribution can raise the energy by at most some $E_0 (= 3 \cdot (14-5)^2)$. (In fact it will be less than that if not all triangles are filled with H's.) The energy of each graph H itself is bounded by some other constant E_1 ($= 54$ plus the contribution from the inserted tree). Thus, upon inserting p graphs H the energy will grow at most by $pE_2 = p \cdot (E_0 + E_1)$.

Summarizing, we see that when we start with m nodes and insert p graphs H we get 3^p graphs of the same energy by rotating the p insertions separately. Furthermore, the order of the graph is $m + 20p$ and the energy is less than $54 + pE_2$, where the 54 is the bound of Lemma 4.1.

One can now rearrange this statement to obtain the claim of Lemma 4.6. Since we started with m nodes and were able to insert at most $2m - 5$ graphs H, each of which adds 20 nodes, we get the inequalities

$$p \leq 2m - 5 \,, \quad n = m + 20p, \quad E \leq 54 + E_2 p, \quad N = 3^p \,.$$

From this we conclude that the inequalities are satisfied if

$$(p+5)/2 \leq m \leq n - 20p \,,$$

that is if $p \leq \frac{2n-5}{41}$ which for large n is satisfied for $p \leq n/25$. This means that the number of insertions for which our construction works is bounded by $n/25$ and the corresponding energy of such graphs is bounded by $54 + E_2 p \leq 54 + E_2 n/25 \leq E_* n$, with E_* for example equal to $E_2/50$ when n is large enough. And in all these cases we have 3^p graphs with the same energy, that is, at least $3^{(E-54)/E_2}$. Introducing the lower bound $E > 100$, we get (4.1) and the proof is complete. □

Remark 4.8. One can obtain somewhat less good bounds by inserting directly christmas trees into each triangle of G_m.

5 The dynamics of defects

A useful way to view a typical state of low energy is the notion of defects. Let us call *defect* any red node whose degree is not 5 and any blue node whose degree is not 7. Thus, the graph of Fig. 7 has 6 defects. When the energy of a triangulation of n nodes is less than εn—which is quite frequent when n is large, as we saw in Lemma 4.6—then there are very few defects, since each costs at least one unit of energy. Therefore, at these very low energies it is useful to view the triangulation as a dilute gas of defects.

Here we want to show that these defects can actually move. Again, this is illustrated by an example. In Fig. 9, we show a sequence of 3 flips with the property that after the flips, one node

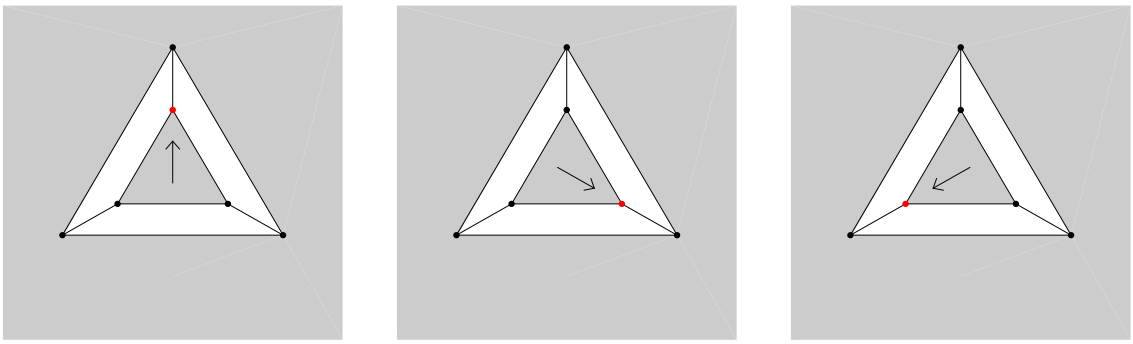

Fig. 8. Three configurations, in the interior of an arbitrary triangle, which have the same energy (the inserted figure being one with three external nodes of same degree and same color). These three configurations are different unless the interior triangle has 3-fold symmetry.

has degree lowered by 1 and a node at distance 2 has degree raised by one, while all other nodes have the same degrees before and after the flips. It is easy to see that this mechanism allows one to "move" a defect by 2 steps with a small number of flips. Of course, by Lemma 2.1 and Lemma 3.2, we already know that this can be done in $\mathcal{O}(n^2)$ steps. But what is new here is that the number of steps needed to move the defect by a distance 2 is independent of the size of the triangulation.

Note that since defects can move, they can actually collide and annihilate each other. In Sect. 7, we will argue how this fits nicely into a random walk picture, of a gas of annihilating defects combined with a rate of spontaneous generation of new defects.

6 Numerical results

6.1 Time evolution of energy

We ran several simulations on triangulations of size $n = 367$, 1096 and 3283. The energy was defined as in Eq. (1.1). All runs have been done starting from a fixed initial configuration, with fixed temperature. The original triangulation is obtained by starting from a tetrahedron which is recursively subdivided by the insertion of tetrahedra. Thus, at level ℓ of recursion there are $4 + \sum_{i=1}^{\ell} 3^i$ nodes. Our runs are for levels 5 to 7.

In Fig. 10 we illustrate the typical scenario for the evolution of the energy as a function of the number of flips, at temperature $T = 0.175$. After a short initial phase, there is a marked decrease of the energy until it reaches an order of about 100 (for the sizes of our triangulations). Then a slow decay sets in until an equilibrium value is reached.

The absolute time scales seem proportional to n. So we can produce a first data collapse by rescaling time by a factor $3283/n$. This is done in Fig. 11.

Glassy slowing down is demonstrated in Fig. 12. Here we concentrate on the phase just before equilibrium is reached. With very good quality, one finds an exponential slowing down. The energy behaves like the logarithm of the number of flips. More precisely, before saturation, we find laws of the form (between $3 \cdot 10^8$ and $3 \cdot 10^{10}$ flips):

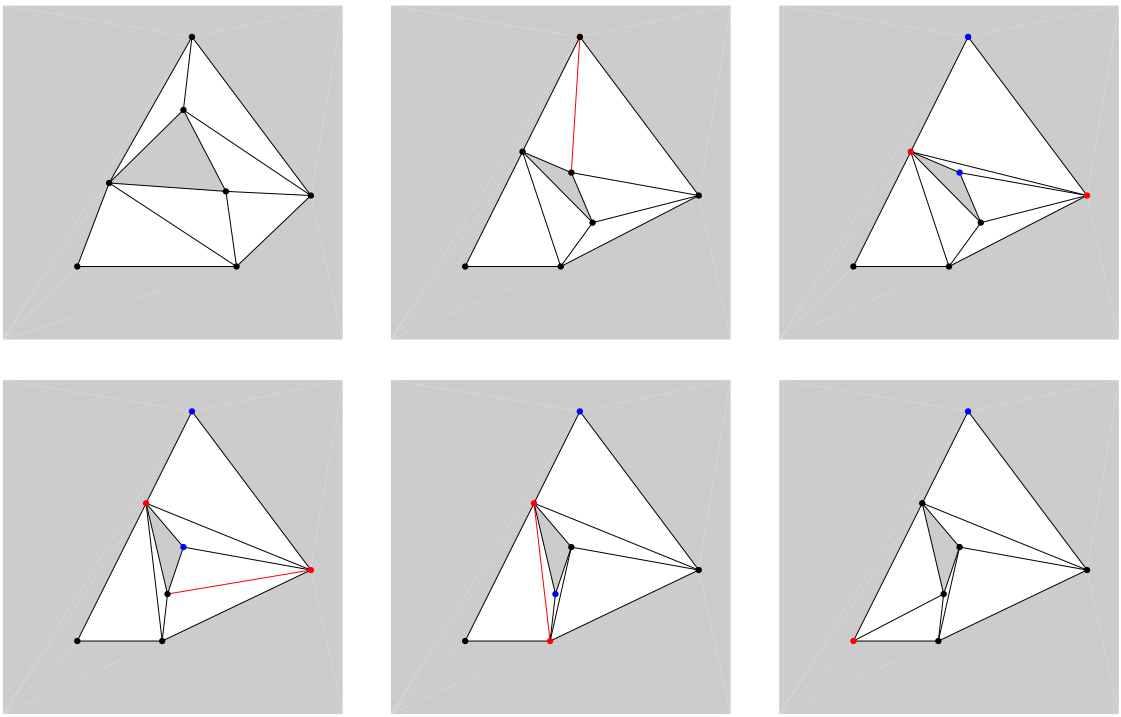

Fig. 9. Motion of a defect by successive flips. Shown is a sequence of moves which lowers the degree by 1 on the top node and raises the degree by one on the bottom left node, leaving in the end all other degrees intact. Flips take only place between frames 2-3, 4-5, and 5-6. The color code of the nodes is red for an increase of the degree by 1 and blue for decrease by one.

$$\begin{aligned}(E_{367}-6)/367 &= 0.44958 - 0.01897\log(3283/367\cdot\text{flips})\,,\\ (E_{1096}-6)/1096 &= 0.46169 - 0.019362\log(3283/1096\cdot\text{flips})\,,\\ (E_{3283}-6)/3283 &= 0.44554 - 0.18652\log(\text{flips})\,.\end{aligned} \tag{6.1}$$

The correlation coefficients of these fits increase from 0.977 to 0.997.

Remark 6.1. The minimal energies we have seen at $T = 0.175$ are summarized in Table 1.

n	4 instead of 5	5	6 instead of 5	6 instead of 7	7	8 instead of 7	total energy
367	6	178	0	5	178	0	11
1096	10	536	2	4	544	0	16
3283	8	1629	5	11	1627	3	27

Table 1. Some states with very low energy which have been found in the simulations. The numbers indicate the number of nodes of given degree. After the first column we give the counts for the red nodes (which want to have degree 5) and then for the blue nodes (which want to have degree 7).

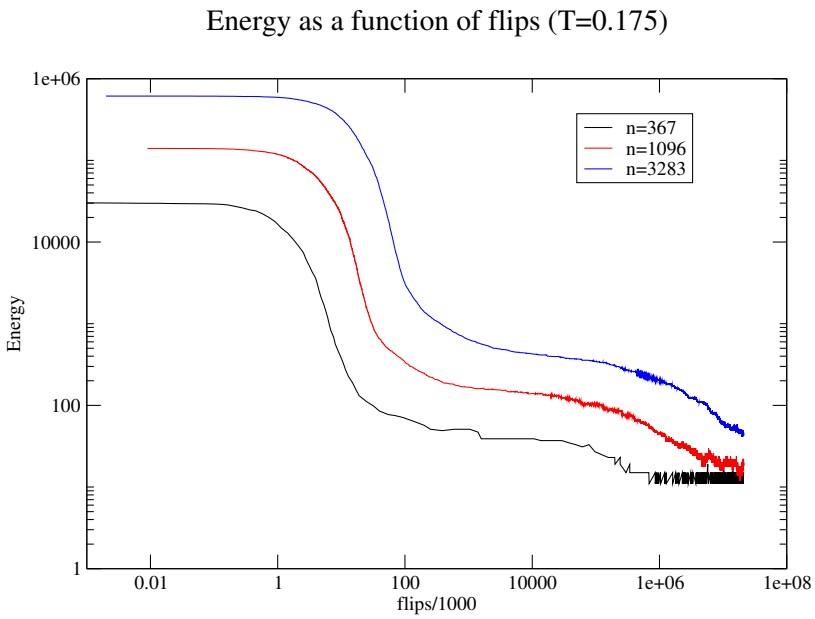

Fig. 10. The energy as a function of the number of flips. The vertical scale is energy.

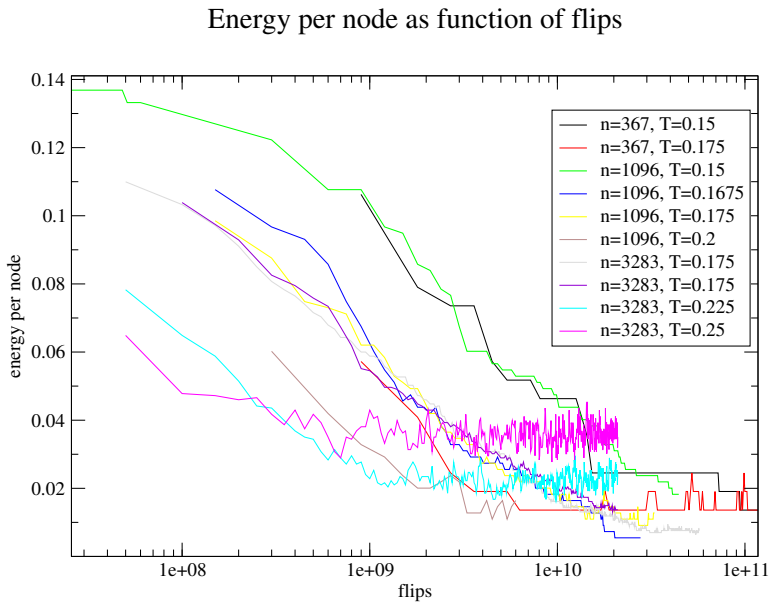

Fig. 11. The data for $n = 367$, 1096, and 3283 and $1/\beta = T$ as shown in legend. The x axis is the logarithm of number of attempted flips, normalized by $3283/n$, and the y axis energy per node after having subtracted a zero-point energy $E_0 = 6$ from all the energies. Note a certain data collapse for each temperature T, independent of size n.

6.2 Local minima and the ultrametric property

We have also studied the local neighborhood of typical triangulations (at $T = 0.175$). The results are shown in Fig. 13. The question we answer here is as follows. Take a "typical" low-energy

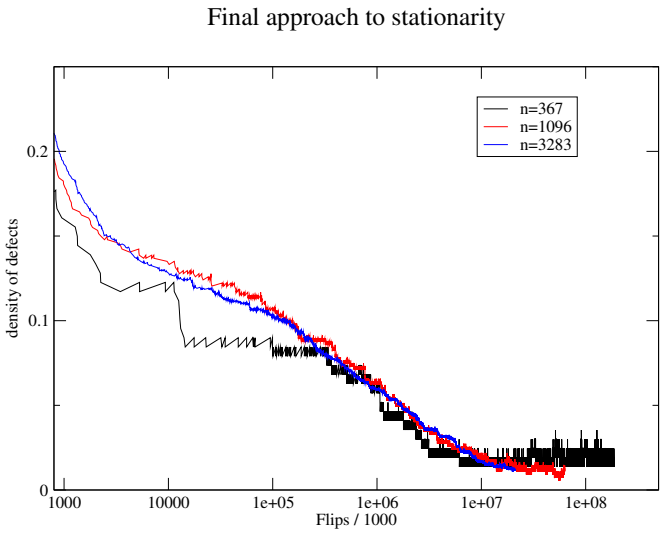

Fig. 12. The energy as a function of the number of flips on approach to equilibrium. The vertical scale is density of defects, *i.e.*, defects/nodes. The horizontal axis is the number of flips, renormalized by $3283/n$, *i.e.*, the smaller triangulations converge faster than the larger ones. However, the *slope* is the same for the 3 cases. We have subtracted 6 from the energies, to take into account the 0 point energy (which is at least 6).

triangulation and compute for every possible flip starting from this triangulation the change of energy δE which that flip would generate. For a triangulation with n nodes there are in general $3n-6$ possible choices of the edge which is going to be flipped, as discussed in Sect. 3. The figure shows the number of these flips which change the energy by $\delta E = -2, 0, \ldots, 10$, averaged over 200–700 states (depending on n). The values are expressed as probabilities. In fact, the fluctuations between samples are very small and basically every single sample has the same distribution. Also note that this distribution is largely independent of the size of the system, except that very rare events are absent in the smaller triangulations.

In terms of the energy landscape on the graph $\mathcal{G}$ of Sect. 3 this means that every point on $\mathcal{G}$ which is a typical glass state is almost a local minimum. In almost 100% of all directions (flips) leaving a given point, the energy grows by 4, with fewer and fewer directions with different growth. Only about 0.0004 of all directions are energy neutral, and the probability to find a direction in which the energy *decreases* is only about $6.6 \cdot 10^{-7}$. This means that the probability to find a saddle point (increase and decrease of energy possible) for $n = 3282$ is only about 0.002. In other words, only about 1 in 500 of the sampled states is not a local minimum, but actually a saddle. One can understand these numbers by observing that flipping a link in a region where the four affected nodes have the "right" degree (namely, either 5 or 7, depending on color) will cost 4 units of energy. Since most nodes have this property in the stationary state, a gain of four is the normal situation. The much rarer other energy changes are possible if a link is flipped in a region

with a defect, and those are very rare. It should be possible to quantify all this as a function of temperature, *i.e.*, as a function of the density of defects.

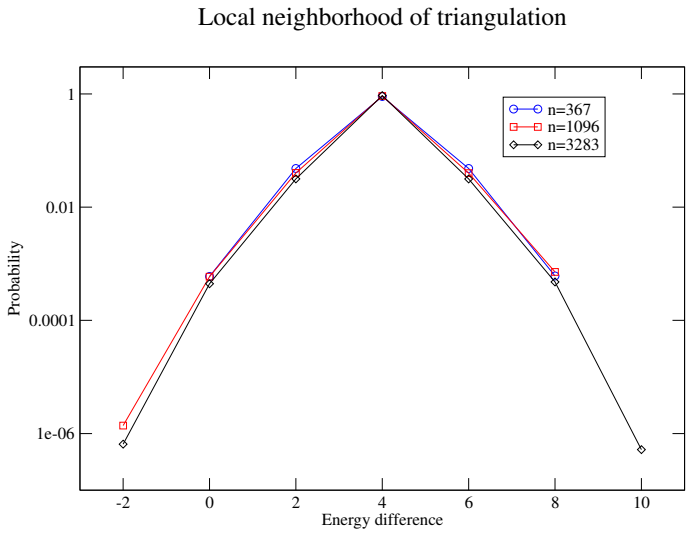

Fig. 13. The neighborhood of typical glassy configurations. See the text for explanations.

One can push this picture somewhat further and show that the local minima are relatively deep. Indeed, to study the local neighborhood we looked at all possible movements from the current state to its $3n - 6$ neighbors (or slightly less when there are tetrahedra around). Note now that the next choice of a link for the next motion will, with high probability, affect nodes which were *not* touched in the first move. Therefore, with high probability, there is another increase of energy by 4 units for this second step. This can go on for many more flips. For example, if we do another $n^{1-\varepsilon}$ flips, with $\varepsilon > 0$, then they will all imply (with high probability) new nodes, and each such step will increase the energy by 4. Thus, the local minima are in troughs at least $4n^{1-\varepsilon}$ deep (with very few directions with less increase). So the local minima are surrounded by walls at least $4n^{1-\varepsilon}$ high, in most directions. Note that this fact is intimately related to the topology of the graph $\mathcal{G}$.

Thus, the following picture emerges, leading to the familiar ultrametric scenario. Any state with very few defects is basically a local minimum. Only very well-chosen "exit" directions from such a state do not increase the energy. Going two steps away from the original state, the probability of finding an exit without energy increase is approximately the square of that finding such an exit when doing one state. And this picture will repeat for a number of $o(n)$ steps, so that each local minimum is surrounded by walls of height $o(n)$ and exits of probability $\mathcal{O}(1/n)^k$ without increase of energy in k steps (and probability $\mathcal{O}(1/n)^{k-\ell}$ for an energy increase of 4ℓ). Note that these observations depend only on the short range behavior of the energy function, in our special case, the constant 4, but not on the large scale growth of, say $(d_i - 5)^2$. One expects that these local

minima will become equilibrium states, and this is how the ultrametric property appears in this model.

6.3 Temporal correlations

Here we present some measurements of temporal correlations. By this one means that one compares the triangulation at time t to triangulations at time $t + \delta t$ (it is well-known that this is the right aging approach, see *e.g.*, [2]. The distance $D(\mathcal{T}, \mathcal{T}')$ between two triangulations $\mathcal{T}$ and $\mathcal{T}'$ is defined as the number of (numbered) nodes which have different degrees or different neighbors.[1] This measure is mathematically not quite right, since two triangulations which only differ in a renumbering of the nodes (respecting color) would be considered equal in $\mathbb{T}_n$ but unequal here. The advantage of the current definition is that it is very easy to implement. (A better measure would be the minimum of the distance over all permutations of the numbering of the nodes, or the shortest distance between $\mathcal{T}$ and $\mathcal{T}'$.) These quantities are illustrated in Figs. 14 and 15.

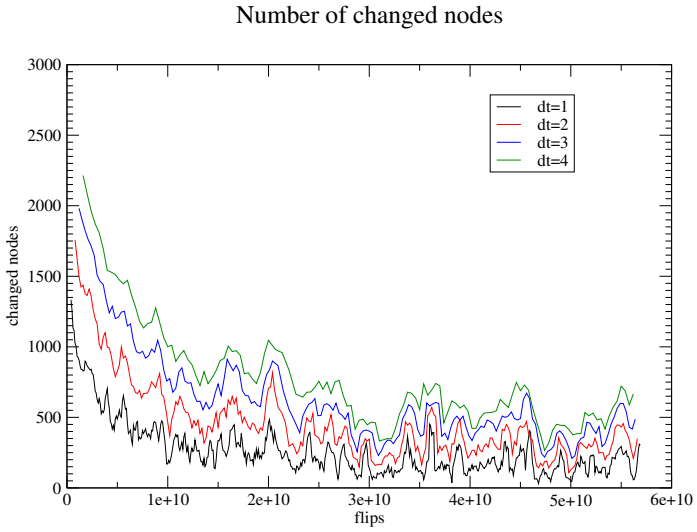

Fig. 14. Number of nodes which *differ* between time t (in flips) and time $t + 10^8 \cdot dt$. The data are for $n = 3283$ and $T = 0.175$.

[1] More precisely, we represent the triangulations by fixing a certain numbering of nodes, and by enumerating for each node its neighbors in counter clockwise order. When doing comparisons, we compare these representations, as obtained in the simulations.

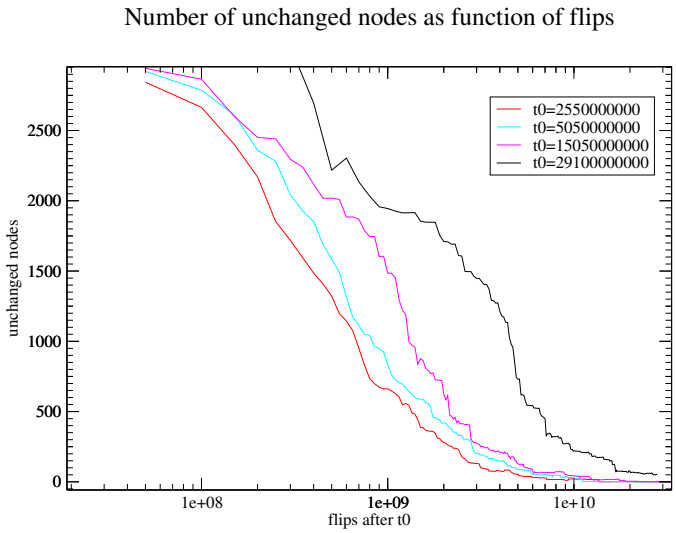

Fig. 15. Number of nodes which are *unchanged* as a function of dt. The vertical axis is $3283 - D(t_0, t_0 + dt)$, with t_0 given in the caption and D defined in the text. The data are for $n = 3283$ and $T = 0.175$.

6.4 Spatial correlations

Here, we compare two spatial correlations, one for the regular torus triangulation, and the other for a state of the triangulation taken towards the end of the run. These correlations are measured with a technique known from quantum gravity (with dynamical triangulations of S^4), see [4]. The correlation function $C(r)$ at distance r is defined as

$$C(r) = \frac{\sum_{ij:\mathrm{dist}(i,j)=r}(d_i - \bar{d})(d_j - \bar{d})}{\sum_{ij:\mathrm{dist}(i,j)=r} 1} \,,$$

where d_i is the degree at i, $\bar{d}$ is the mean degree, and the distance between two nodes i and j is defined as the minimal number of hops to get from i to j. The power spectrum is then the amplitude of the Fourier transform of this quantity.

In Fig. 16 we show that the power spectrum of the regular triangulation has, as expected, a peak, while the one for the glassy phase shows no structure at all. The precise data are as follows: The torus triangulation is regular as described in Remark 4.4, with 0 energy, and 3600 nodes. The glassy triangulation is a typical state of a simulation done with 3283 nodes, at temperature $T = 0.175$.

7 A random walk interpretation

Glass models can be classified in largely two different classes, and, at present it is not clear whether these two classes are the same or are different. The first class can be called the “deep valley” class.

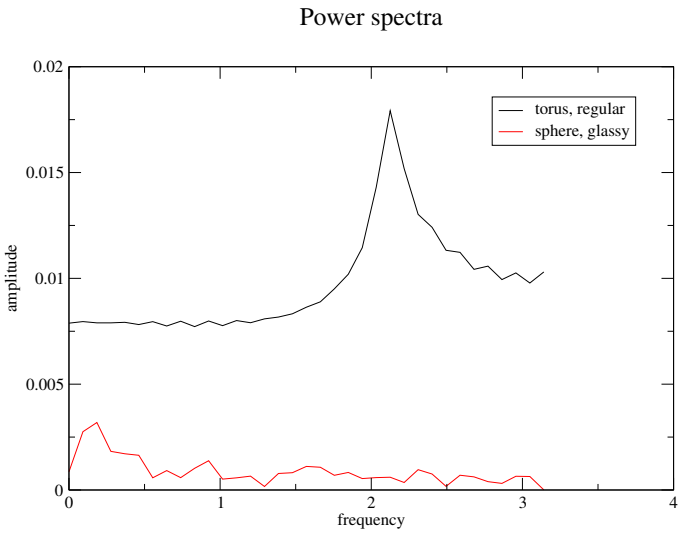

Fig. 16. Power spectra for the torus triangulation and a glassy triangulation, corresponding to the equilibrium at $T = 0.175$.

People imagine a landscape with increasingly deep valleys and the random walk enters them, and, the deeper the valley one finds, the harder it is to get out of the valley to find eventually an even deeper one. The second class can be called "narrow corridors" class. Here, the valleys are rather flat, and, while the shortest distance between two points might be quite short, it might be very difficult to find a path which has a small total variation in height, going from one configuration to another. The model in [1] and this one seem to be of this second class.

How should one view our the model at very low temperature? Most odd (blue) nodes will have a degree 7 while most even (red) ones have degree 5, if the temperature is low enough. Furthermore, there will be a density of "defects" that is, odd ones of degree different from 7 and even ones of degree different from 5, as seen in Table 1. Experimentally, what happens is that at low temperature only 6's and 8's occur for the odd ones and 4's and 6's for the even ones. We can thus view these defects (which all cost energy 1 each) as a gas of low density. At a given temperature, 4 defects are usually created by flipping an edge in a region with no defects (all 4 corners will acquire a "wrong" degree). One new defect can be created when one flips a link which connects to only one old defect. The probability of this happening (per flip) is proportional to $\exp(-4\beta)$ (resp. $\exp(-2\beta)$.) Thus, 4- (or 2-) tuples are randomly created at this rate. On the other hand, defects can wander (painfully) through the triangulations as we have shown above in Sect. 5. When 2 or 4 of them meet they can annihilate, and the final density of defects as a function of β should be obtainable as the equilibrium between creation and annihilation of these defects. Note that, since annihilation lowers the energy, this will happen with a rate 1 whenever they meet, while creation happens with the much smaller rate $\exp(-4\beta)$.

Remark 7.1. Our discussion of defects differs from that of [1]. In that paper, most particles live, at low temperature, in a hexagon. Any red particle in a pentagon (or blue particle in a 7-gon) is then called a *glass-defect*, while all other cases are called *liquid-defects*. In contrast, in our model the natural thing is to have red particles in pentagons and blue ones in 7-gons, and defects are any coordination numbers different from 5 or 7. In particular, a hexagon is a defect in our model. Given our earlier discussion, at the temperatures we consider, all defects which appear in the simulations would correspond to glass-like defects. The following discussion can the be seen as a variant of Eqs. (2) and (3) in [1].

7.1 A toy model

One can study the density of defects in a simplified model which is basically exactly solvable[2]. The model is as follows: Take a square lattice (sublattice of $\mathbb{Z}^2$) of size $N \times N$ with periodic boundary conditions. Each site of the lattice can be either empty or filled with one particle. Fix a constant ϱ (this mimics $\exp(-4\beta)$). The Markov process consists in choosing at random one of the sites.

1. If it is filled, move the particle randomly in one of the 4 directions to the next site. If the target site is occupied, the particles annihilate each other. If not, the particle stays at the new site.
2. If the site is empty, create a new particle there with probability ϱ.

The conjecture is that the equilibrium density of the particles, for $N \to \infty$ and small ϱ, should behave like

$$\text{const.}\varrho^{1/2}|\log \varrho|^{1/2} \,. \tag{7.1}$$

Remark 7.2. We have checked this law for $N = 100$, with a very good fit (see Fig. 17).

The connection between this model and our model of a glass is almost obvious. The migration of defects was discussed in Sect. 5, see also Fig. 9. The only difference here is that moves in the glass model are slower, since perhaps the energy will increase on the way from a position to the next. But this only changes the time scale of the moves of defects. The creation of defects takes usually place either in a region where there is no defect nearby, and then the energy increases by 4, hence the probability of this happening will be $\exp(-4\beta)$. But perhaps other such creations will only need energy 2, and this is not covered by the toy model. The toy model is on a lattice $\mathbb{Z}^2$ while the defect model is on the triangulation —not on the set $\mathbb{T}_n$ of triangulations—since we talk here about motion of defects, viewed as *independent*, unless they collide. Therefore, what can be reasoned on $\mathbb{Z}^2$ transposes to the triangulation, since both are locally transient. Therefore, we conjecture that for the topological glass model, the density of defects should behave like (7.1), with ϱ of the form $\varrho = \exp(-\beta C)$, for some C. We have not been able to verify this in the simulations.

Coalescing and annihilating random walks are discussed in various places, see *e.g.*, [9].

[2] Yuval Peres and Bernard Derrida kindly explained to me how one discusses such models, and also suggested the precise law.

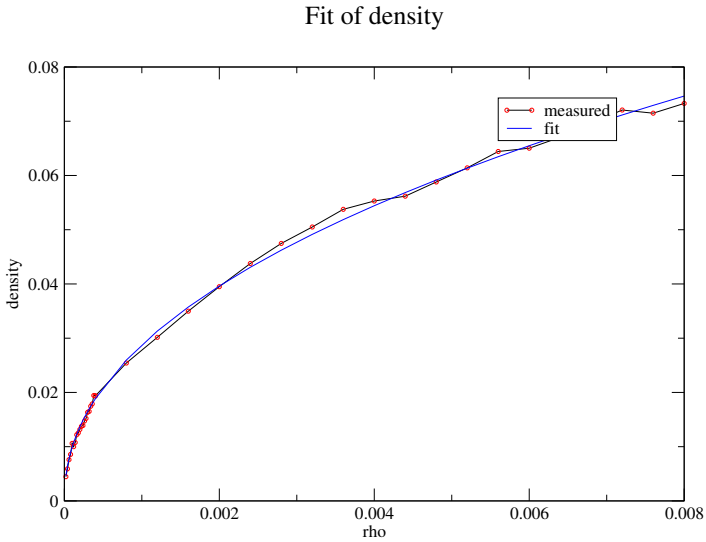

Fig. 17. The asymptotic density of walkers for the model of Sect. 7.1 as a function of the temperature. The theoretical curve is $f(\varrho) = a\varrho^{1/2}|\log(b \cdot \varrho)|^{1/2}$ with $a = 0.252$ and $b = 0.00217$.

8 Conclusions and outlook

In this paper, we have discussed a variety of properties of a glass-like model. These properties show that the glass-like behavior can be obtained without reference to position, but already in a discrete phase space (given by the graph $\mathcal{G}$ of triangulations and their connections through flips). Furthermore, the energy landscape and its concomitant slowing down of motion to equilibrium, seem to depend mostly only on the cost of *local* energy changes, and are thus universal. The *global* structure is in fact hard-wired into the graph $\mathcal{G}$. It would be interesting to see whether the equilibrium states can be mapped back into a physical space, for example by mapping the triangulation onto the disk in such a way that every point is away from every other point by at least the same minimal distance r, and to compare the result to those obtained with classical potentials.

Acknowledgement. We have profited from very useful discussions with G. Ben Arous, B. Derrida, Th. Giamarchi, N. Linial, Y. Peres, and I. Procaccia. This work was partially supported by the Fonds National Suisse.

References

1. E. Aharonov, E. Bouchbinder, H. G. E. Hentschel, V. Ilyin, N. Makedonska, I. Procaccia, and N. Schupper. Direct identification of the glass transition: Growing length scale and the onset of plasticity. *Europhysics Letters* **77** (2007), 56002.

2. G. Ben Arous and J. Černý. Dynamics of trap models. In: A. Bovier, F. Dunlop, A. van Enter, and J. Dalibard, eds., *Mathematical Statistical Physics, Les Houches, Session LXXXIII* (Elsevier, 2006).
3. P. Collet and J.-P. Eckmann. Dynamics of triangulations. *J. Stat. Phys.* **121** (2005), 1073–1081.
4. B. de Bakker and J. Smit. Gravitational binding in 4d dynamical triangulation. *Nucl. Phys. B* **484** (1997), 476–492.
5. V. A. Malyshev. Probability related to quantum gravitation: planar gravitation. *Uspekhi Mat. Nauk* **54** (1999), 3–46.
6. R. Mori, A. Nakamoto, and K. Ota. Diagonal flips in Hamiltonian triangulations on the sphere. *Graphs Combin.* **19** (2003), 413–418.
7. S. Negami. Diagonal flips of triangulations on surfaces, a survey. In: *Proceedings of the 10th Workshop on Topological Graph Theory (Yokohama, 1998)*, volume 47 (1999).
8. W. T. Tutte. A census of planar triangulations. *Canad. J. Math.* **14** (1962), 21–38.
9. J. van den Berg and H. Kesten. Asymptotic density in a coalescing random walk model. *Ann. Probab.* **28** (2000), 303–352.
10. K. Wagner. Bemerkungem zum Vierfarbenproblem. *Jber. Deutsch. Math-Verein.* **46** (1936), 126–132.
11. D. J. Watts and S. H. Strogatz. Collective dynamics of small-world networks. *Nature* **393** (1998), 440–442.